CHAPTER 5

Computational Investigation on Molecular Interactions between the DNA Binding Domain of p53 and Acidic Domain of MDM2

Computational Investigation on Molecular Interactions between the DNA Binding Domain of p53 and Acidic Domain of MDM2

5.1. Abstract:

The tumour suppressor p53 molecule is primarily negatively regulated by the MDM2 protein. The primary site of interaction between p53 and MDM2 has been well studied. But there exists a secondary site of interaction between the DBD of p53 and central AD of MDM2, which aids to the stability of the complex. Here, we have studied the conformational dynamics and stability of the p53(DBD)-MDM2(AD) complex using molecular dynamics (MD) simulation. We have also determined the protein-protein interaction (PPI) profile for the complex. The interface area involved in the interaction were found to be 1119 $Å^2$ and 1056 $Å^2$ for p53(DBD) and MDM2(AD) respectively. The MD simulation results highlight the significance of salt bridges and hydrogen bonds in the stability of the p53(DBD)−MDM2(AD) complex. We also carried out the BFE as well as PRED analyses for the complex. A good binding affinity between p53 (DBD) and MDM2 (AD) was found (-17.22 kcal mol^{-1}). The findings from our highlight the noticeable structural as well as binding characteristics of the p53(DBD)−MDM2(AD) complex, that may be beneficial in designing novel potential inhibitors for the proper disruption of the p53(DBD)-MDM2(AD) interactions.

5.2. Introduction:

A key protein that suppresses tumour growth is p53. It controls the differentiation, cell death, as well as cell proliferation of cells. Numerous cellular stressors, such as oncogene activation, DNA damage, hypoxia, as well as replicative stress, cause the p53 protein to become active [587]. Posttranslational modifications are a component of the activation mechanism that prevent MDM2 from destroying p53 and increase the DNA-binding affinity of p53. When active, p53 tetramers bind to responsive regions in genomic DNA, triggering the transcription of a number of target genes that control tumour suppression, stress tolerance, DNA repair, cell cycle arrest, and apoptosis [588]. Approximately 50% of human cancers have p53 mutations. New functions that promote tumour growth replace the mutant p53's transcriptional activity [589].

There are numerous structural and functional domains in the p53 protein. The NTD, which has 90 residues, is made up of two TADs (TAD1: 1-40, TAD2: 40-60), which are followed by a proline-rich area (PRR: 60–90) [589]. The main MDM2 protein binding site is present in TAD1. TAD2 is necessary for both protein interactions and transcription activation. Mutations in TAD1 and TAD2 are required to stop the tumor-suppressing activity [590]. The p53 TAD1 and TAD2 include a large number of phosphorylation sites that control both the activity and degradation of p53 during the stress response. PRR with mutations or deletions impair apoptosis, transactivation, p53 degradation, tumour suppression, and growth inhibition [591-593]. Sequence-specific DNA binding requires the presence of the central DBD (residues: 94-312). The majority of cancer's point mutations also have it as their target. An oligomerization domain (OD: 323-355) and a lysine-rich C-terminal tail (CTD: 364-393), that contains acetylation, methylation, and phosphorylation sites, make up the C terminus (CT: 312-393).

Figure 5.1. *Structure of p53 with the major domains. Taken from [596].*

The main p53 negative regulator MDM2 demonstrates both p53-dependent and p53-independent activities. Through its domain architecture, MDM2's features are made clear. The interaction with p53 and blocking its transcriptional activation depend on the N-terminal region. The linker region which follows the NTD consists of a nuclear localization signal (NLS) at residue 178 and a nuclear export signal (NES) at residue 192. An essential auxiliary role in the degradation of p53 is played by the central AD [594-596]. Next is the zinc-finger domain, which is thought to facilitate interactions with a variety of proteins, including the tumour suppressor p14ARF and nucleolar and ribosomal proteins [597]. A nucleolar localization signal (NoLS; comprising of residues 466–473) is part of the RING (Really Interesting New Gene) domain, which is made up of amino acids 436–482. The MDM2 C terminus is made up of the RING domain in addition to the residues found in the tail of the C terminus (amino acids 485–491). Interactions between RING domains are significantly influenced by the C terminal tail [598, 599]. The E3 ligase activity of MDM2, which is necessary for the protein to limit the p53 molecules

throughout early embryogenesis, depends on the RING domain of the protein.

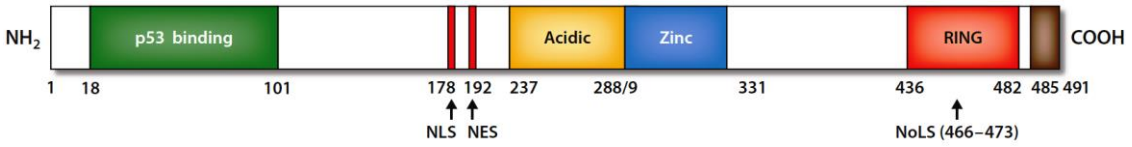

Figure 5.2. *Structure of MDM2 with the major domains. Taken from [596].*

Between the molecules p53 and MDM2, there is a mutual regulation that is kept in place by a feedback loop [600]. The transcription rate for the MDM2 mRNAs & proteins increases when any stimulus or DNA damage activates p53 molecules. This leads to the interaction of MDM2 with p53, which directly limits the activity of p53 molecules through three main methods. The p53 molecules are first ubiquitinated by MDM2 (an E3 ligase), which causes their proteasomal destruction. Second, the MDM2(NTD) binds to p53's TAD1, which is the key site of binding between p53 and MDM2, preventing p53 from connecting to its target DNA, which prevents transcription. Third, the nuclear target DNA required for transcription is unable to access the p53 molecules because they are quickly exported from the cell's nucleus by the MDM2 molecules. Significantly, it has been discovered that amplification of the MDM2 gene and mutations in the tumour protein 53 (*TP53*) do not coexist in human malignancies.

In addition to their major interaction site, the molecules p53 and MDM2 also interact at a secondary location. This additional interaction takes place between the core DBD of p53 and the core central AD of MDM2. Furthermore, this interaction is necessary to target p53 for effective ubiquitination [601-606].

In the present study, the conformational dynamics and stability of the p53(DBD)-MDM2(AD) complex has been studied using molecular dynamics (MD) simulation. BFE and PRED analyses were also carried out to infer the binding characteristics and identify hotspot residues across the interface of the p53(DBD)-MDM2(AD) complex. The protein-protein interaction (PPI) profile has been studied using online server.

5.3. Materials & Methods:

5.3.1. Preparation of the p53(DBD)-MDM2(AD) system:

The 3D structure of MDM2(AD) has been modelled using the FASTA sequence of Human MDM2 protein retrieved form UniProt database (UniProt ID: Q00987), and then submitting the FASTA sequence (residues: 237-288) to the I- TASSER server. I-TASSER has reportedly been rated as the top automated protein prediction server by the CASP ranking. Five models were obtained. The C-score, which was derived from the relative clustering structural density and consensus significance, was used to determine the optimum model. Template modelling (TM) score and RMSD are used to assess the correctness of the optimum model. The best (optimum) structure was then visualized using the UCSF Chimera software v.1.13.1.

The 3D structure of the DBD of p53 has been downloaded from RCSB PDB (PDB ID: 2FEJ). The modelled 3D structure of MDM2 (AD) is then docked with the 3D structure of p53 (DBD) using ClusPro 2.0 online server. The complex structure with the best model score was chosen as the initial structure for the further analyses.

5.3.2. MD simulation of p53(DBD)-MDM2(AD) complex:

The p53(DBD)-MDM2(AD) system was prepared for the molecular dynamics (MD) simulation using the AMBER ff99SB force field using the Leap module of the AMBER 14 software package. The rest of the steps were performed as mention in section **4.3.2**.

5.3.3. Analysis of the MD Trajectories:

Using the PTRAJ (short for Process TRAJectory) and CPPTRAJ (a rewrite of PTRAJ in C++) modules of AMBER 14 Tools, we then analysed the MD trajectories for the p53(DBD)-MDM2(AD) complex. To assess the convergence of our system, the RMSD for p53(DBD), MDM2(AD), and p53(DBD)-MDM2(AD) complex were studied, wherein the starting structure of MD was used as the reference. RMSF was calculated to analyze the flexibility of the complex. We also performed the Rg, SASA, intra/inter-molecular hydrogen bond analyses for the system to understand how the p53(DBD)-MDM2(AD) complex stability is getting affected during the entire course of MD simulation.

5.3.4. Determination of the interface residues:

In order to determine the protein-protein interaction profile of the p53(DBD)-MDM2(AD) complex. The lowest potential energy structure of the p53(DBD)-MDM2(AD) complex was extracted using RMSD clustering algorithm. The lowest energy structure of the complex was then uploaded in the PDBsum server in order to visualize the interacting interface residues of the p53(DBD)-MDM2(AD) complex. The protein residues whose contact center of mass (CoM) distances from its interacting protein partner are less than 6 Å are called the interface residues.

5.3.5. BFE analysis for the p53(DBD)-MDM2(AD) complex:

The BFE and PRED of the p53(DBD)-MDM2(AD) complex interface residues were calculated using the procedure mentioned in section **4.3.6.**

5.4. Results & Discussions:

5.4.1. Analysis of the conformational changes of the p53(DBD)-MDM2(AD) complex throughout the course of MD Simulation:

MD simulations provide in-depth knowledge about the dynamic characteristics of a specific system under study, and assist us in understanding changes in their flexibility and stability with respect to time.

The snapshots of the p53(DBD)-MDM2(AD) complex structure were created from the MD trajectories of the 80 ns simulation, at intervals of 20 ns using UCSF Chimera (as shown in **Figure 5.3**).

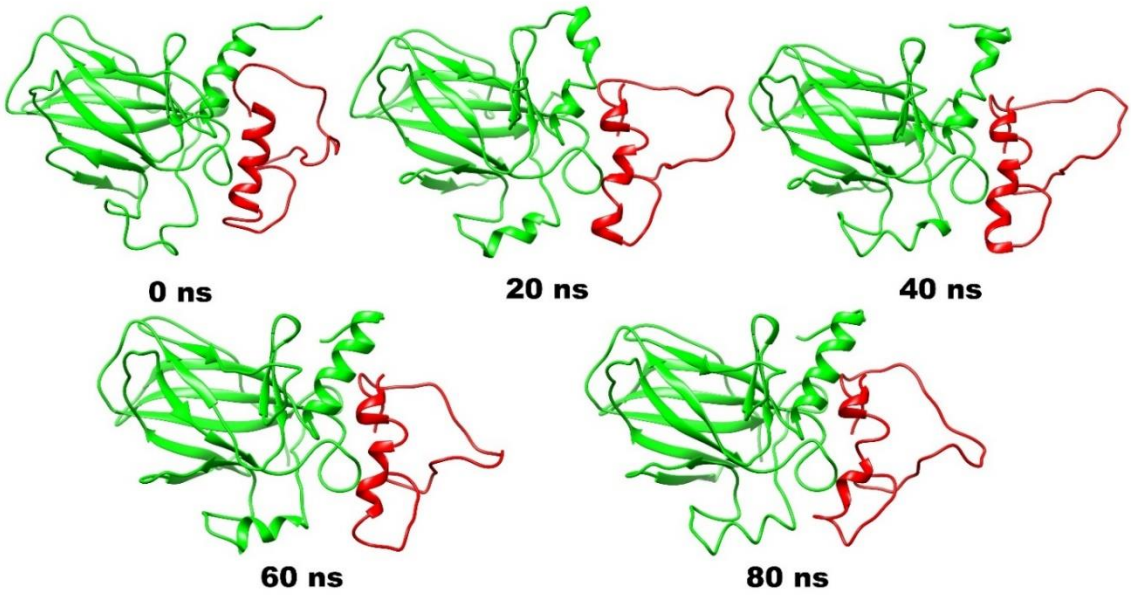

Figure 5.3. *Representative conformation of p53(DBD)-MDM2(AD) complex throughout the MD simulation of 80 ns.*

5.4.2. DSSP analysis of the p53(DBD)-MDM2(AD) complex:

We then carried out the DSSP analysis using the Kabsch and Sander algorithm in order to study the variations in secondary structural elements in p53 and MDM2 molecules. **Figure 5.4a** depicts the secondary structural changes in p53(DBD) molecule. **Figure 5.4b** represents the secondary structural changes in MDM2(AD) molecule. From **Figure 5.4a**, it can be seen that there is a large proportion of anti-parallel and parallel sheets, along with some α-helix in p53(DBD) throughout the entire course of simulation. From **Figure 5.4b**, it can be seen that there is a large proportion of α-helix in MDM2(AD) throughout the entire course of simulation. Both α-helices and beta sheets provide better stability to protein structures. Hence, the p53(DBD)-MDM2(AD) complex is found to have good stability throughout the simulation.

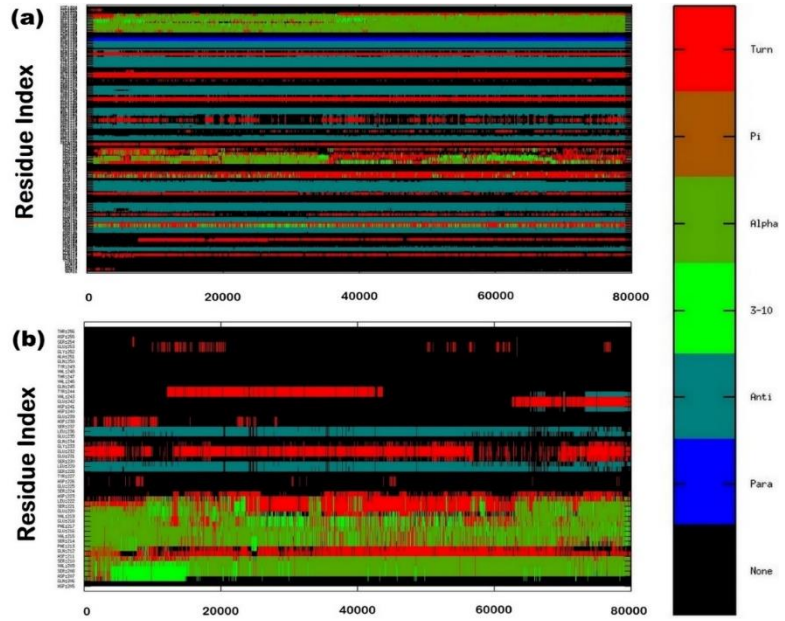

Figure 5.4. *Dictionary of Secondary Structure of Proteins (DSSP) analysis for (a) p53(DBD), and (b) MDM2(AD). The secondary structure components are color-coded as shown in the panel.*

5.4.3. Analysis of probable secondary structure per residue of p53(DBD) and MDM2(AD) in the p53(DBD)-MDM2(AD) complex:

Then we performed the analysis of the probable secondary structure for each residue of p53 and MDM2 can adopt throughout the simulation. **Figure 5.5a** corresponds to the probability score versus residue index for the p53 molecule. **Figure 5.5b** corresponds to the probability score versus residue index for the MDM2 molecule. From **Figure 5.5a**, we observe that the p53(DBD) molecule contains the secondary structure anti-parallel sheets predominantly, followed by alpha-helix (the last few residues). From **Figure 5.5b**, we see MDM2(AD) molecule to contain α-helix and anti-parallel sheets predominantly.

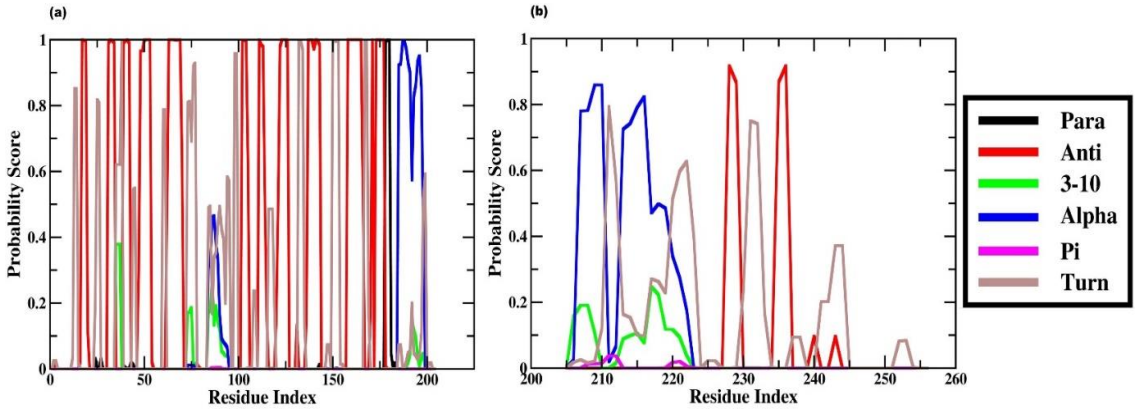

Figure 5.5. *Probability score for secondary structure analysis for (a) p53(DBD), and (b) MDM2(AD).*

5.4.4. RMSD Analysis of the p53(DBD)-MDM2(AD) complex:

In a usual MD simulation, the stability of the system is usually determined by the RMSD of the protein/biological molecule with respect to time. For the p53(DBD)-MDM2(AD) complex studied, the RMSD values with respect to time have been shown in **Figure 5.6a**. **Figure 5.6a** represents a comparative RMSD plot for the p53(DBD), MDM2(AD), and p53(DBD)-MDM2(AD) complex. The p53(DBD), MDM2(AD) and p53(DBD)-MDM2(AD) complex was found to have converged at 36 ns with the average CoM distance of 4 Å, 4 Å, and 4.5 Å, respectively.

5.4.5. RMSF Analysis of the p53(DBD)-MDM2(AD) complex:

Residue flexibility of the p53(DBD)-MDM2(AD) system was assessed using the RMSF. **Figure 5.6b** represents the RMSF values for C-α atoms of the individual p53 and MDM2 molecules in the p53(DBD)-MDM2(AD) complex with respect to the time evolution of 80 ns trajectories. For the p53(DBD)-MDM2(AD) complex, the residue fluctuations were noticed throughout entire MDM2(AD), and residue fluctuations were observed for N-terminal and C-terminal residues of the p53(DBD). Comparing the RMSF of the p53(DBD) and MDM2(AD) with the p53(DBD)-MDM2(AD) system, more number of average residue fluctuations can be observed in MDM2(AD) than in p53(DBD).

5.4.6. Rg Analysis of the p53(DBD)-MDM2(AD) complex:

Rg is generally calculated to determine the overall dispersion of atoms in a biomolecule from their common center of gravity/axis. The Rg analysis for p53(DBD), MDM2(AD), and p53(DBD)-MDM2(AD) complex are shown in **Figure 5.6c**. Here, it can be observed that the Rg values for the p53(DBD), MDM2(AD), and p53(DBD)-MDM2(AD) to fluctuate within the mean value of 17 Å, 13 Å, and 19.5 Å, respectively. The curves for p53(DBD), MDM2(AD), and p53(DBD)-MDM2(AD) were observed to be settled during the entire course of simulation (production dynamics).

5.4.7. SASA Analysis of the p53(DBD)-MDM2(AD) complex:

The overall changes in the total SASA of p53(DBD), MDM2(AD), and p53(DBD)-MDM2(AD) are shown in **Figure 5.6d**. The SASA values are analogous, as well as are directly reflective of the inappropriate (hydrophobic) contacts between the biomolecules and the water molecules. To determine the surface area accessible by the solvent (water) for the p53(DBD)-MDM2(AD) complex, a probe of radius of 1.4 Å was used. The SASAs of the p53(DBD), MDM2(AD) and p53(DBD)-MDM2(AD) complex were found to be constant at 12000 $Å^2$, 5000 $Å^2$, and 15000 $Å^2$ respectively. Thus, the greater the number of residues, the greater the number of hydrophobic interactions available, and greater will be the SASA value.

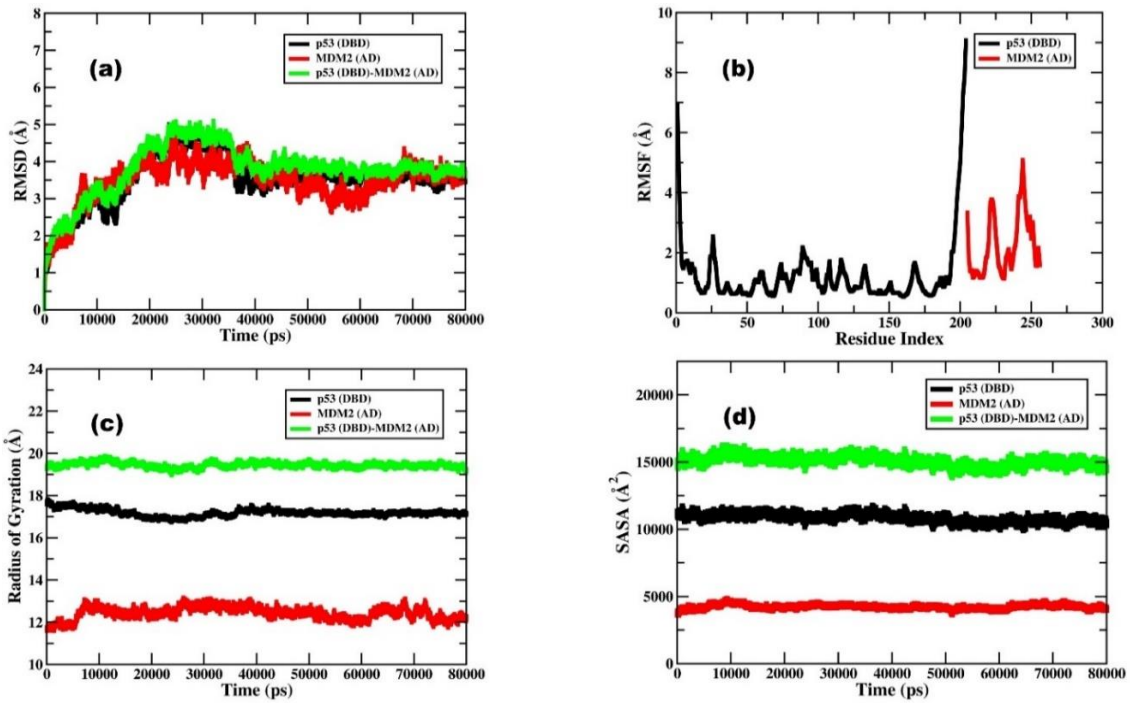

Figure 5.6. *The structural characteristics (a) Root Mean Square Deviation (RMSD), (b) Root Mean Square Fluctuation (RMSF), (c) Radius of Gyration (Rg), and (d) Solvent Accessible Surface Area (SASA) of p53(DBD), MDM2(AD), and the complex during 80 ns Molecular Dynamics simulation.*

5.4.8. Hydrogen Bond Analysis of the p53(DBD)-MDM2(AD) complex:

The number of intramolecular hydrogen bonds present in p53(DBD) and in MDM2(AD), and the number of intermolecular hydrogen bonds existing in the p53(DBD)-MDM2(AD) complex were also calculated, as the hydrogen bonds play a significant role in providing the stability to the protein complexes. The hydrogen bonds found were shown in **Figure 5.7** and were observed to have the values within the optimal range recommended for globular proteins. An average of eighty hydrogen bonds was found to be present in p53(DBD) (**Figure 5.7a**), an average of fifteen hydrogen bonds was found to be present in MDM2(AD) (**Figure 5.7b**), an average of ten inter-molecular hydrogen bonds was found to be present in the p53(DBD)-MDM2(AD) complex with p53(DBD) as donor and MDM2(AD) as acceptor (**Figure 5.7c**), and an average of four inter-molecular hydrogen bonds was found to be present in the p53(DBD)-MDM2(AD) complex with MDM2(AD) as donor and p53(DBD) as acceptor (**Figure 5.7d**).

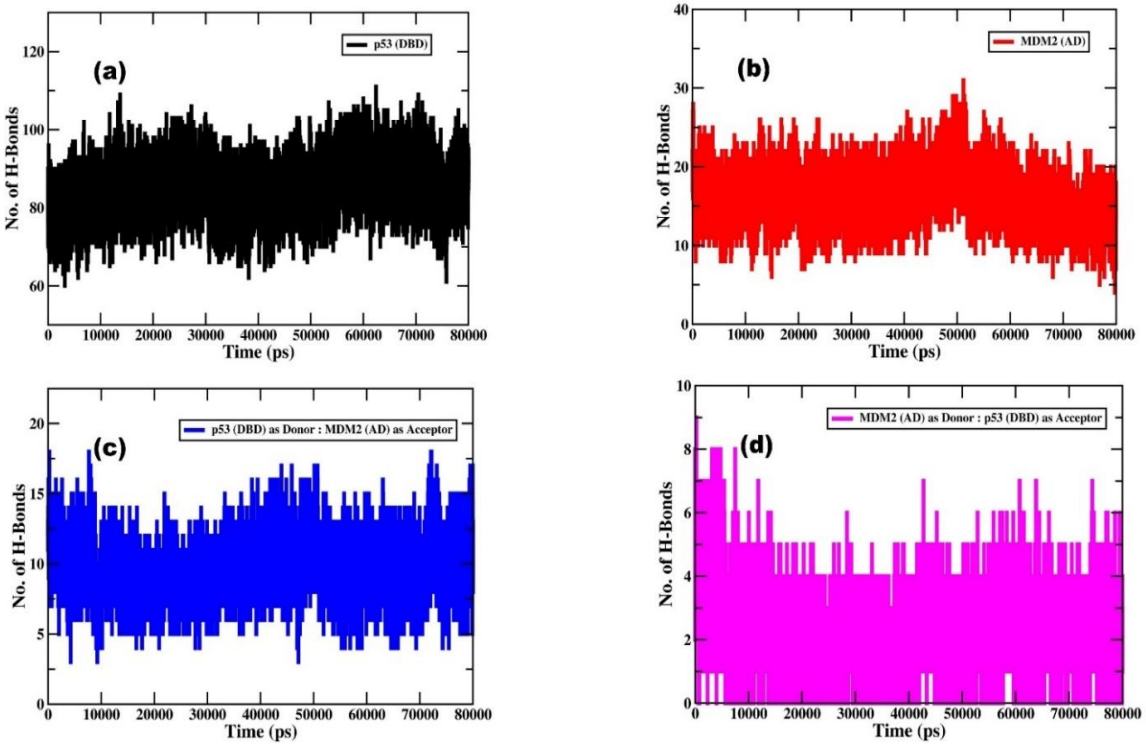

Figure 5.7. *Intra-molecular hydrogen bond analysis of (a) p53(DBD), and (b) MDM2(AD); and intermolecular hydrogen bond analysis for the p53(DBD)-MDM2(AD) complex structure, where (c) p53(DBD) is donor and MDM2(AD) is acceptor, and (d) MDM2(AD) is donor and p53(DBD) is acceptor.*

5.4.9. Determination of the interface interactions of the p53(DBD)-MDM2(AD) complex:

An interface area is often described as an area where two sets of proteins get into contact with one another. They are generally characterized by the surface residues with quite large surface areas accessible to the available solvent. When the lowest energy structure of the p53(DBD)-MDM2(AD) complex retrieved using the RMSD Clustering algorithm from the 80 ns MD trajectories was submitted to the PDBsum server, the interface statistics for the p53(DBD)-MDM2(AD) complex were generated. **Table 5.1** represents the interface statistics. The intermolecular interactions between p53(DBD) and MDM2(AD) of the p53(DBD)-MDM2(AD) complex have been summarized at the residue levels in **Figure 5.8**. The p53(DBD)-MDM2(AD) complex has forty interface residues in total. The interface area for p53(DBD) and MDM2(AD) chains that were involved in the interaction were found to be 1119 $Å^2$ and 1056 $Å^2$ respectively. Molecular interactions such as hydrogen bonding, salt bridges, and non-bonded contacts helped to stabilise the docked complex. From **Figure 5.8**, it can be observed that one hundred sixty non-bonded interactions are present along with four salt bridges and fourteen hydrogen bonds between p53(DBD) and MDM2(AD), which contribute to the stability of the p53(DBD)-MDM2(AD) complex. Twenty-two residues from p53(DBD) and eighteen residues from MDM2(AD) and are found to be involved in the interaction between p53(DBD) and MDM2(AD).

Table 5.1. *Interface statistics for the lowest energy structure of the p53(DBD)-MDM2(AD) complex.*

Chain	No. of Interface Residues	Interface Area ($Å^2$)	No. of Salt Bridges	No. of Disulphide Bonds	No. of Hydrogen Bonds	No. of Non-Bonded Contacts
MDM2	18	1119	4	-	14	160
p53	22	1056				

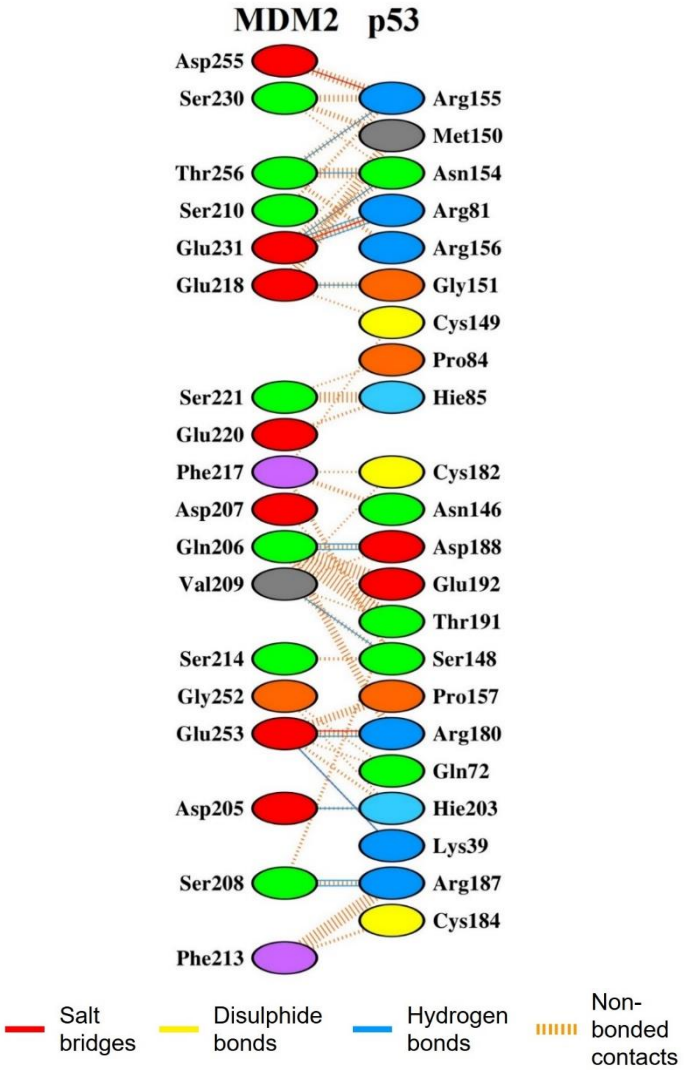

Figure 5.8. *Intermolecular interactions between MDM2(AD) and p53(DBD) in the lowest energy structure of the p53(DBD)-MDM2(AD) complex.*

5.4.10. BFE and PRED analyses of the p53(DBD)-MDM2(AD) complex:

The BFE of p53(DBD) and MDM2(AD) to form the p53(DBD)-MDM2(AD) complex was calculated using the MM-GBSA method. The BFE calculated for the p53(DBD)-MDM2(AD) complex, along with the various energy terms, are shown in **Table 5.2**.

Table 5.2. *The various components of the BFE (kcal mol^{-1}) evaluated by MM/GBSA method in p53(DBD)-MDM2(AD) complex.*

Components	**Complex (kcal mol^{-1})**	**Standard Deviation (±)**	**Receptor (kcal mol^{-1})**	**Standard Deviation (±)**	**Ligand (kcal mol^{-1})**	**Standard Deviation (±)**	**$\Delta\Delta G_{binding}$ (kcal mol^{-1})**	**Standard Deviation (±)**
$\Delta E_{VDWAALS}$	-1830.53	23.05	-1482.21	18.60	-248.91	7.37	-99.42	5.01
ΔE_{EL}	-15457.29	46.71	-12865.10	33.21	-198.86	25.60	-2393.33	34.01
ΔE_{GB}	-5380.02	35.43	-2559.27	31.43	-5246.78	20.97	2426.03	31.03
ΔE_{SURF}	107.74	0.95	83.69	0.91	39.53	0.53	-15.48	0.31
ΔG_{gas}	-17287.82	47.40	-14347.31	32.81	-447.76	24.08	-2492.74	32.71
ΔG_{solv}	-5272.28	35.24	-2475.58	31.64	-5207.26	21.16	2410.55	31.04
ΔG_{TOTAL}	-22560.10	37.25	-16822.89	32.78	-5655.02	14.78	**-82.19**	5.39
TS_{TRA}	16.87	0	16.66	0	15.45	0	-15.25	0
TS_{ROT}	17.41	0.01	17.01	0	15.22	0.04	-14.82	0.04
TS_{VIB}	2835.04	6.25	2256.96	7.28	612.99	3.50	-34.90	9.13
TS_{TOT}	2869.31	6.25	2290.63	7.278	643.65	3.53	**-64.97**	9.14
$\Delta G_{binding}$							**-17.22**	

$\Delta E_{VDWAALS}$ = van der Waals contribution from MM; **ΔE_{EL}** = electrostatic energy as calculated by the MM force field; **ΔE_{GB}** = the electrostatic contribution to the polar solvation free energy calculated by GB; **ΔE_{SURF}** = non-polar contribution to the solvation free energy calculated by an empirical model; **ΔG_{gas}** = total gas phase energy (**ΔE_{gas} = $\Delta E_{ele} + \Delta E_{vdW}$)**; **$\Delta G_{solv}$** = sum of nonpolar and polar contributions to solvation; **ΔG_{TOTAL}**= final estimated binding free energy in kcal mol^{-1} calculated from the terms above (**ΔG_{TOTAL}= $\Delta G_{gas} + \Delta G_{solv}$**); **$TS_{TRA}$** = translational energy; **TS_{ROT}** = rotational energy; **TS_{VIB}** = vibrational energy; **TS_{TOT}** = total entropic contribution; and BFE (**$\Delta G_{binding}$**).

From **Table 5.2**, it can be observed that all the derived components for the BFE analysis contributed to the binding of p53(DBD) and MDM2(AD) to form the p53(DBD)-MDM2(AD) complex. The $\Delta G_{binding}$ for the p53(DBD)-MDM2(AD) complex gives a value of -17.22 kcal mol^{-1}.

For the better understanding of the protein-protein binding process, the contribution of each individual residue to the BFE has been studied in depth. To create the residue-residue interaction spectrum, the BFE has been decomposed in terms of interacting residue-residue pairs. The residue decomposition process is particularly effective for describing the protein-protein binding mechanism at the atomic level, as well as analysing the contribution of each individual residue to the BFE. The contribution of numerous key residue-residue pairs toward BFE is split into vdW energy, the sum of electrostatic energy and polar solvation energy, and non-polar solvation energy, as per the analytic results of

the residue-residue interaction spectrum. The results for the total energy from each residue have been shown in **Figure 5.9**. From the analysis, it can be observed that MET243, ARG273, ARG174, and ASN247 from p53(DBD), and residues GLU263, GLN238, and PHE249 from MDM2(AD) make a substantial contribution towards the BFE.

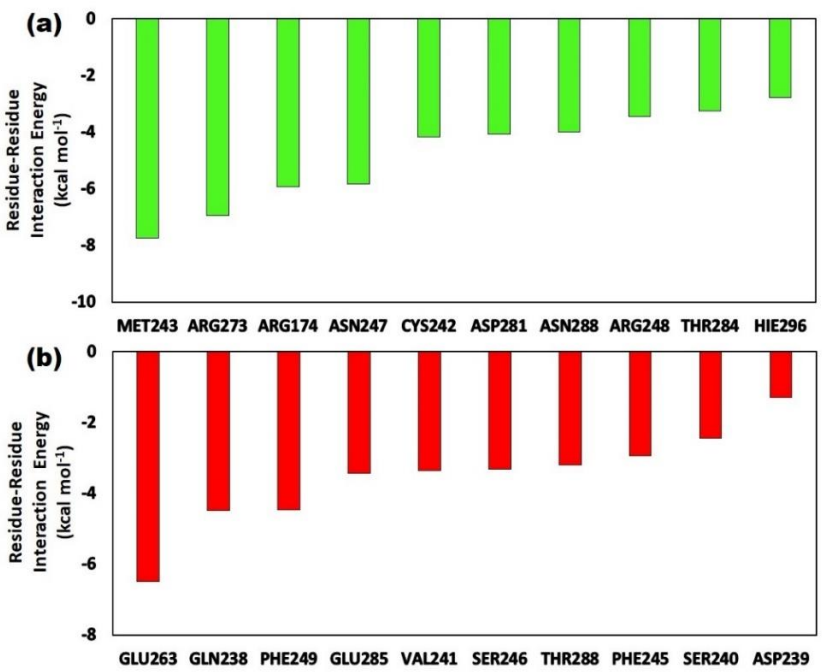

Figure 5.9. *PRED analysis for (a) p53(DBD) and (b)MDM2 (AD).*

5.5. Conclusion:

In this work, we have studied the stability and the conformational dynamics of the p53(DBD)-MDM2(AD) complex. The stability of the complex was determined using RMSD analysis. The p53(DBD)-MDM2(AD) complex retained its stability from 36 ns of the MD simulation. From the secondary structure analysis for the complex, it was found that both p53(DBD) and MDM2(AD) predominantly contains α-helix as well as β-sheets, which aid in better stability of the complex. We also found four salt bridges and fourteen hydrogen bonds to be the crucial factor for the stability of the complex. The binding affinity between p53(DBD) and MDM2(AD) was found to be quite high ($\Delta G_{binding}$ = -17.22 kcal mol^{-1}). A significant number of interface residues (MET243, ARG273, ARG174, and ASN247 from p53(DBD), and residues GLU263, GLN238, and PHE249 from MDM2(AD)) make a substantial contribution towards the binding affinity of the complex. Our findings may be useful for designing potential inhibitors that disrupt all the interactions between p53 and MDM2 molecules.